Journal of Applied Polymer Science

# Effects of fiber-surface treatment on the properties of hybrid composites prepared from oil palm empty fruit bunch fibers, glass fibers, and recycled polypropylene

**Muhammad Remanul Islam,[1] Arun Gupta,[1] Makson Rivai,[1] Mohammad Dalour Hossen Beg,[1] Md. Forhad Mina[2]**

[1]Faculty of Chemical and Natural Resources Engineering, Univerisiti Malaysia Pahang, Lebuhraya Tun Razak, Gambang 26300, Kuantan, Malaysia

[2]Department of Physics, Bangladesh University of Engineering and Technology, Dhaka, Bangladesh

Correspondence to: M. R. Islam (E-mail: remanraju@yahoo.com)

**ABSTRACT:** In this article, we report the effects of hybridization and fiber-surface modification on the properties of hybrid composites prepared from recycled polypropylene (RPP), coupling agents, oil palm empty fruit bunch (EFB), and glass fibers through a twin-screw extruder and an injection-molding machine. The surface of the EFB fibers was modified with different concentrations (10–15 wt %) and temperatures (60–90°C) of alkali solutions. The structure and morphology of the fibers were observed with the help of Fourier transform infrared spectroscopy and scanning electron microscopy. Different types of composites were fabricated with untreated, alkali-treated, and heat-alkali-treated fibers. Comparative analysis of the mechanical, structural, morphological, and thermal properties of the composites was carried out to reveal the effects of treatment and hybridization. The analysis results reveal that composites prepared from the alkali-treated (in the presence of heat) fibers show improved mechanical, thermal, and morphological properties with a remarkably reduced water absorption. Additionally, the crystallinity of RPP also increased with the development of biaxial crystals. The improvement of various properties in relation to the structures and morphologies of the composites is discussed.
 J. Appl. Polym. Sci. **2016**, *133*, 43049.

**KEYWORDS:** composites; crystallization; fibers; thermogravimetric analysis (TGA); thermoplastics

Received 15 April 2015; accepted 14 October 2015
**DOI: 10.1002/app.43049**

## INTRODUCTION

Natural fibers have been used as promising reinforcements in polymer composites for a few decades in the manufacture of valuable structural materials. Among these fibers, jute, silk, kenaf, sisal, and flax have been used as important reinforcing agents for improving the mechanical and thermal properties of polymeric composites.[1–4] Because of their low density, low cost, high specific properties, environmentally friendliness, biodegradability, and ready availability, natural fibers are important materials for their potential applications in composite industries.[5] Despite these advantages, natural fibers possess some negative features, such as a high moisture absorption, poor compatibility with the polymer matrix, vulnerability to attack by microbes and fungi, and UV degradability.[6] These problems can be overcome by fiber-surface modifications through physical and chemical treatments or with different coupling agents or compatibilizers. With these techniques, the interfacial adhesion between the fibers and the polymer is improved; this results in good mechanical, thermal, structural, and morphological properties in the composites.[7–9] For instance, a coupling agent, such as maleic anhydride, is often used to enhance the adhesion between the fibers and the polymer matrix.[10,11] Fiber-surface modification through alkali solution or ultrasound has also been found to be very useful because it is a low-cost technique compared to the use of compatiblizers.[6,7]

Recently, hybridization with more than one fiber to get double or multiple effects simultaneously on the properties of composites has also attracted researchers' attention. Various synthetic fibers, such as glass, aramid, and carbon fibers, have been used together with natural fibers as reinforcing agents in the preparation of polymer composites.[12–14] The simultaneous effect from both types of fibers can be used to alter the thermal, mechanical, structural, and morphological properties of hybridized fiber-reinforced composites. In a previous work, an increase in the mechanical properties of aramid-fiber- and glass-fiber (GF)-reinforced polymer composites, as compared to those in the

virgin polymer, was reported.[1,2] Additionally, the water absorption properties of composites prepared with aramid-fiber-based flax–epoxy resin was found to be reduced because of hybridization.[1]

In the fabrication of a hybrid composite (HC), the proportional ratio of different fibers is important. In a previous study, the optimization of the fiber content was performed for recycled polypropylene (RPP), GF, and oil palm empty fruit bunch (EFB) fibers.[15] In this study, a comparative study of the effects of the hybridization of GFs and alkali-treated or heat-aided alkali-treated EFB fibers on the performances of recycled polymer composites was carried out. Generally, the properties of recycled-materials-based polymers are not similar than pure or virgin polymers. The properties usually deteriorate because of degradation and further processing. Therefore, the results of the use of recycled materials are most often discouraging, and hence, their use has been losing interest in the production of useful products. They also have a negative impact in terms of high cost during the recycling process and additional additives. Moreover, environmental issues and legislation restrict them from being dumped in soil and open places. Therefore, the use of recycling-based materials needs further study for the preparation of valuable composite materials to add some value to them and encourage recycling. Interestingly, some good results have been observed from the previous data, where the results with recycling-based materials were impressive, with similar properties to those of pure or virgin-based materials.[16,17] For that reason, this article deals with RPP, which was made from used bumper and battery casings of vehicles.

The aim of this study was to fabricate hybridized-fiber-reinforced RPP produced from high-loaded EFB fibers (treated by alkali and heated-alkali solutions) and low-loaded GFs to obtain the maximum benefit. It is noteworthy that oil palm EFBs are abundantly available and annually renewable fibers in southeast Asian countries, especially in Malaysia. The best utilization of these biobased materials could reduce the volumetric occupancy and add value to some products.

## EXPERIMENTAL

### Materials

RPP [density = 0.91 g/cm$^3$ and melt flow index (MFI) = 5.58 g/10 min] and GF (density = 2.56 g/cm$^3$) were purchased from a local company, Alva Suplayer Sdn. Bhd. (Kuantan, Malaysia). EFB fibers were kindly supplied by Lepar Hilir Palm Oil (Pahang, Malaysia). Polybond 3200 (PB; density = 0.91 g/cm$^3$ and MFI = 115 g/10 min) was purchased from Eastman Chemical Sdn. Bhd. (Kuantan, Malaysia). Fusabond P 613 (FB; density = 0.903 kg/m$^3$ and MFI = 120 g/10 min) was purchased from DuPont. NaOH was procured from Merck (Germany).

### Fiber Processing and Treatments

The EFB fibers were washed with normal water for 2 h to remove mud and other surface impurities and then dried in sunlight for 2 days. The dried fibers were then soaked in alkaline solution (10, 12.5, or 15 wt %) for 2 h at ambient temperature. The dried raw fibers were also treated with a 12.5 wt % NaOH solution at three different temperatures (60, 75, and 90°C) for 2 h. Thus, three types of fibers were obtained individually from the alkali and heated-alkali treatments. All six different types of treated fibers were washed thoroughly with normal water to remove the adhered NaOH solution from the surface of the fibers. The removal of alkali from the fiber surface was confirmed by the pH value of 7 of the washed water. The treated fibers were cut with a crusher machine and passed through a sieve to obtain uniform lengths from 2 to 4 mm. GFs were also cut into lengths of 2–4 mm and heated at 450°C for 2 h to remove the sizing agents. The abbreviations for the different fibers are listed in Table I.

### Composite Preparation

The shredded EFB fibers were dried at 80°C in an oven overnight and compounded with GF, RPP, and coupling agents (PB and FB) with a twin-screw extruder (Prism Eurolab 16) and then injection-molded with an injection-molding machine (NESSEI, model PNX60) at 190°C. The fiber content was fixed as 40 wt %, where the EFB to GF ratio was maintained at 70:30. The amount of RPP and coupling agents (PB and FB) used were 57.5 and 2.5 wt %, respectively. The abbreviations of all of the samples produced in this study are given in Table I.

### Characterization

**Density.** A gas pycnometer (Micrometrics AccuPyc II 1340) was used to determine the density of the fibers and composites. This equipment was operated by inert helium gas. The densities of five replicates from each category of samples were measured, and an average value of these was considered for analysis.

**MFI.** The MFI of each sample was determined with a Dynisco melt flow indexer (LMI 4000 series), according to ASTM D 1238 (heating temperature = 230°C, applied load = 2.16 kg). An average of three runs was considered for each sample.

**Tensile Testing.** Tensile testing was conducted according to ASTM D 638-03. The specimens were tested with a Shimadzu (model AG-1) universal testing machine (load cell = 5kN, crosshead speed = 5 mm/min, and gauge length = 50 mm). The test was performed until tensile failure occurred. Five specimens were tested for each batch, and their average value was considered for analysis.

**Fourier Transform Infrared (FTIR) Spectroscopy Analysis.** The functional groups of the EFB fibers were analyzed by FTIR spectrometry (THERMO model) with the standard KBr pellet technique. Each spectrum was recorded at wave numbers ranging from 4000 to 500 cm$^{-1}$.

**Flexural Testing.** Flexural testing was conducted according to ASTM D 790-97 method. A universal testing machine (Shimadzu, model AG-1) with a static load cell of 1 kN was used for the measurement. The support and crosshead speed were fixed at 20 mm and 10 mm/min, respectively. Five specimens were tested, and the average value was considered for the analysis.

**Izod Impact Testing.** Izod impact testing was performed according to ASTM D 256. A universal pendulum impact system (Ray-Ran, United Kingdom) with a hammer of load 0.163 kg and a swing speed of 3.5 m/s was used for testing. A

**Table I.** Abbreviations of the Samples Used for Analysis

| Sample name | Abbreviation |
|---|---|
| Raw EFB fibers | REFB |
| EFB fibers treated at 25°C with a 12.5 wt % NaOH solution | AEFB |
| EFB fibers treated at 90°C with a 12.5 wt % NaOH solution | HAEFB |
| RPP | RPP |
| Raw-EFB-fiber-based composites | NFC |
| GF-based composite | GFC |
| HC based on REFB and GF | HC |
| HC (EFB treatment conditions: 10.0 wt % NaOH at 25°C) | HC1 |
| HC (EFB treatment conditions: 12.5 wt % NaOH at 25°C) | HC2 |
| HC (EFB treatment conditions: 15.0 wt % NaOH at 25°C) | HC3 |
| HC (EFB treatment conditions: 12.5 wt % NaOH at 60°C) | HC4 |
| HC (EFB treatment conditions: 12.5 wt % NaOH at 75°C) | HC5 |
| HC (EFB treatment conditions: 12.5 wt % NaOH at 90°C) | HC6 |

Ray-Ran motorized notching cutter was used to notch the specimen. The notch depth was fixed at $2 \pm 0.02$ mm with angle of 45°. Five specimens were tested, and their average was considered for the analysis.

**Thermogravimetric Analysis.** Thermogravimetric analysis was carried out with a thermogravimetric analyzer (TA Instruments, model TGA Q-500). A nearly 5-mg sample was weighed and heated from 25 to 600°C at a heating rate of 20°C/min. Thermogravimetric analyses were conducted in a platinum crucible under a nitrogen atmosphere to ensure an inert atmosphere at a flow rate of 40 mL/min.

**Differential Scanning Calorimetry (DSC).** A TA Instruments model DSC Q-1000 was used to perform DSC of the samples in an aluminum pan at a heating rate of 10°C/min. A heat–cool–heat method was applied in the temperature range 25−220°C. The percentage of crystallinity ($\chi_{DSC}$) was obtained with eq. (1)[7]:

$$\chi_{DSC} = \left(\frac{\Delta H}{\Delta H_m W}\right) \times 100\% \quad (1)$$

where $\Delta H$ is the heat of fusion of the sample, $\Delta H_m$ is the heat of fusion of the 100% crystalline polypropylene (PP), and $W$ is the mass fraction of the matrix.

**X-ray Diffraction.** The crystalline properties of the samples were measured by X-ray diffraction analysis. A X-ray diffraction machine (model Rigaku Mini Flex II, Japan) was used for the testing. The tube current and operating voltage were maintained at 15 mA and 30 kV, respectively. The samples were scanned stepwise with 5–40° scattering angles ($2\theta$s) with Cu K$\alpha$ radiation ($\lambda = 1.541$ Å).

**Table II.** Values of the Density, MFI, IS, and Void Content of the Samples

| Sample | $\rho$ (g/cm$^3$) | MFI (g/10 min) | IS (J/m$^2$) | $V_v$ (%) |
|---|---|---|---|---|
| REFB | 1.40 | — | — | — |
| AEFB | 1.47 | — | — | — |
| HAEFB | 1.51 | — | — | — |
| RPP | 0.91 | 5.58 | 26.25 | — |
| NFC | 1.04 | 2.32 | 14.65 | 7.6 |
| GFC | 1.70 | 2.57 | 22.45 | 8.5 |
| HC | 1.07 | 1.82 | 15.87 | 4.9 |
| HC1 | 1.08 | 1.60 | 16.55 | 4.0 |
| HC2 | 1.09 | 1.57 | 17.93 | 3.2 |
| HC3 | 1.09 | 1.55 | 15.23 | 3.1 |
| HC4 | 1.10 | 1.32 | 18.20 | 2.3 |
| HC5 | 1.11 | 0.99 | 18.88 | 1.4 |
| HC6 | 1.12 | 0.97 | 19.37 | 0.5 |

**Scanning Electron Microscopy.** The surface morphology of the fibers was examined with a scanning electron microscope (Zeiss, Japan). A field emission scanning electron microscope (JEOL, Japan) was used to observe the images of the fractured surfaces of the composites. Air-dried samples were fixed to a metal-based specimen holder with double-sided sticky carbon tape. Then, the samples were coated with gold before observation with a vacuum sputter coater to make them conductive.

**Water Uptake (WU).** The tensile specimens were immersed in distilled water for 150 days. We determined WU after an equal interval of time by measuring the weight gain by the composites. The WU percentage was calculated with eq. (2)[3]:

$$\mathrm{WU}(\%) = \left(\frac{w_f - w_i}{w_i}\right) \times 100 \quad (2)$$

where $w_i$ and $w_f$ are the initial and final weights of the sample, respectively.

## RESULTS AND DISCUSSION

### Density

The densities of the fibers are presented in Table II. The densities of the REFB, AEFB, and HAEFB fibers were found to be 1.40, 1.47, and 1.51 g/cm$^3$. We observed that the treatment of the fibers increased the density of REFB. This was probably due to the removal of noncellulosic compounds, such as lignin, wax, and other surface impurities. The removal of these compounds may have caused changes in the structure of the fibers. As a result, the reordering of the cellulose fibers and, because of that, the reduction in the surface volume may have increased the density.[18]

The densities of different HCs are presented in Table II. The densities of NFC, GFC, HC1, HC2, HC3, HC4, HC5, and HC6 were found to increase gradually with fiber loading and treatment condition. This means that both the fiber incorporation and treatment increased the density of the composites. This

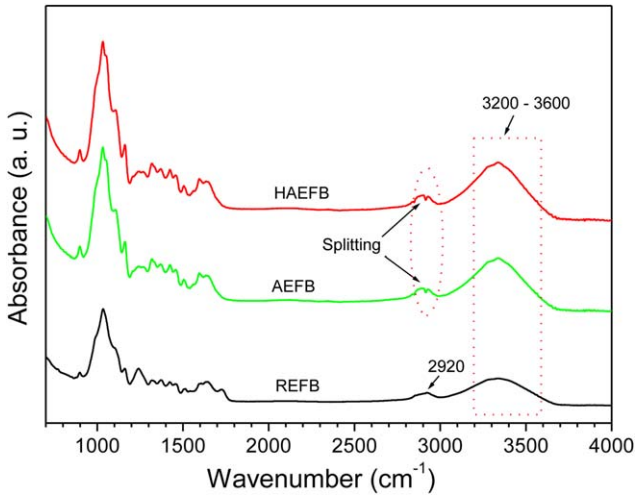


**Figure 1.** FTIR spectra of the REFB, AEFB, and HAEFB fibers. [Color figure can be viewed in the online issue, which is available at wileyonlinelibrary.com.]

increment was probably due to the higher density of the GF and treated EFB fibers. Alkali treatment removed lignin, waxy material, and other surface impurities from the fibers.[7] This treatment made the fiber surface rougher and enabled the fibers to be entangled more compactly in the polymer matrix, whereas a fixed amount of GFs contributed to a constant effect on the density for all of the samples. On the other hand, alkali treatment in the presence of heat enabled the removal of some extra surface materials, whose elimination made the fibers more compact with the polymer; this resulted in the increased densification of the composites. The maximum density was achieved for HC6. Thus, heat-aided alkali treatment showed the maximum effect on the density compared to the fiber treatment by the alkali solution.

### FTIR Spectroscopy of the Fibers

The FTIR spectra of the raw and treated fibers are presented in Figure 1. The intensities of the peaks for the treated fibers were found to be slightly higher compared to the REFB fibers because of the treatment, although some changes were observed in the area of 3200 and 3600 $cm^{-1}$. The peaks in this region are

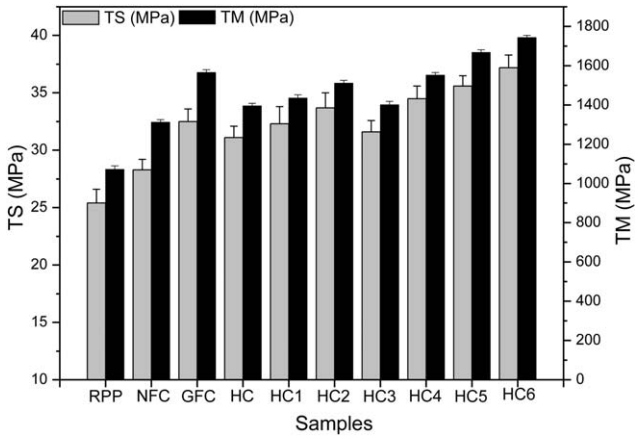


**Figure 2.** TS (MPa) and TM (MPa) of the samples.

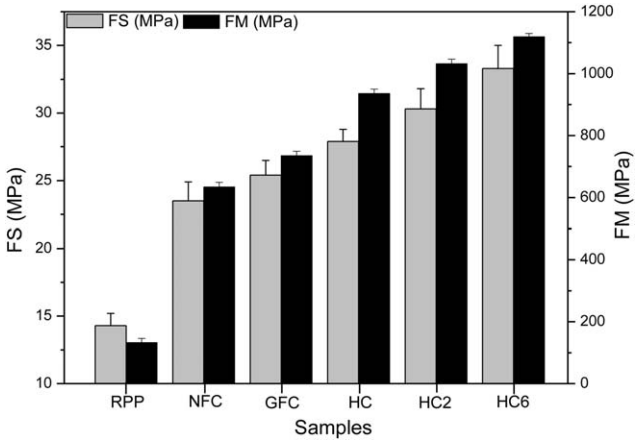


**Figure 3.** FS (MPa) and FM (MPa) of the samples.

usually responsible for the hydroxyl groups of the fibers. The intensities of the curves were found to be high for the AEFB and HAEFB fibers. The absorbance peak around 2920 $cm^{-1}$ was responsible for the stretching vibrations of the methyl and methylene components of the fiber. In the treated fibers, a splitting was observed because of the modification through alkali as a result of the structural changes and removal of noncellulosic compounds. The peak around 1725 $cm^{-1}$ was responsible for the carbonyl (C═O) stretching of acetyl and carboxylic acid components of the hemicellulose and lignin of EFB fibers; this was found to disappear with treatment.[19]

### MFI

The MFIs of different composites are presented in Table II. The maximum MFI was observed for RPP, whereas the loading of fibers decreased the value with a gradual trend. HC2, HC4, HC5, and HC6 contained EFB fibers that were treated at the same concentration of NaOH with gradually increasing temperatures. In a comparison of HC2 and HC6, the MFI of HC6 was found to be decreased by 38%. On the other hand, in a comparison between NFC and HC6, the MFI of HC6 was found to be decreased by 58%. For the case of GFC, MFI was found to be decreased by 54%. The decrease in MFI was found to be up to 3% in comparisons of HC1, HC2, and HC3 to determine the effect of the concentration of NaOH solution at fixed temperature. Thus, the decrease was much higher with treatment temperature compared to the alkali concentration. A low MFI value indicated increased adhesive interaction between the fibers and polymers. Hence, the results indicate that interaction between the fiber and polymer increased more with heated-alkali treatment than with alkali treatment.

### Tensile Properties

The tensile properties, such the tensile strength (TS) and tensile modulus (TM), of the composites are illustrated in Figure 2. We observed that RPP showed TS and TM values of 25.4 and 1072 MPa, respectively. TS and TM were found to be 28.3 and 1312 MPa, respectively, for NFC, whereas GFC showed values of 32.5 and 1565 MPa, respectively. On the other hand, HC exhibited TS and TM values of 31.1 and 1395 MPa, respectively. Thus, the hybridization of EFB fibers and GFs provided an increase in the TS and TM values of the composites. This result

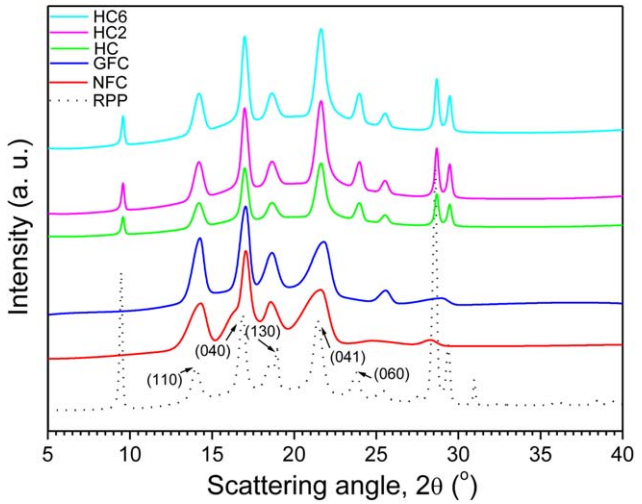


**Figure 4.** X-ray diffraction profiles of the different samples. [Color figure can be viewed in the online issue, which is available at wileyonlinelibrary.com.]

was similar to that of hemp- and GF-based hybrid PP composites, as reported in another article.[20] However, the treatment of fibers with NaOH solution improved the TS to 31.3 and 33.7 MPa for HC1 and HC2, respectively. Similarly, TM was found to be improved to 1395 and 1511 MPa, respectively. After that, the TS and TM values of HC3 were found to be decreased to 31.6 and 1401 MPa, respectively. This deterioration was attributed to the degradation of natural fibers at a high concentration of alkali solution, as noted elsewhere.[7] On the other hand, the TS and TM values of the composites were found to increase gradually with the treatment temperature for a fixed NaOH concentration. The maximum TS (37.2 MPa) and TM (1743 MPa) values were obtained for 12.5 wt % NaOH and 90°C treatment conditions. The TS and TM values of HC6 increased by 46 and 65%, respectively, compared with those of RPP. Thus, both the strength and stiffness of the fabricated composites were found to increase remarkably.

### Flexural Properties

The flexural strength (FS) and flexural modulus (FM) of the composites are shown in Figure 3. The FS and FM values of RPP were found to be 14.3 and 133 MPa, respectively. The FS and FM values of NFC were found to be 23.5 and 634 MPa, whereas the same properties for HC were found to be 27.9 and 935 MPa, respectively. On the other hand, GFC exhibited FS and FM values of 25.4 and 735 MPa, respectively. The properties for HC2 were found to be 30.3 and 1032 MPa, respectively. In comparison among the HCs, the maximum FS and FM values that were achieved were 33.3 and 1119 MPa, respectively, for HC6. The FS and FM values of HC6 increased by 133 and 741%, respectively, compared to RPP. The values were found to be enhanced by 43 and 75%, respectively, compared to those of NFC. These improvements are significant for the uses of HCs. These trends in the mechanical properties of polymeric composites were also noticed in a previous study.[20]

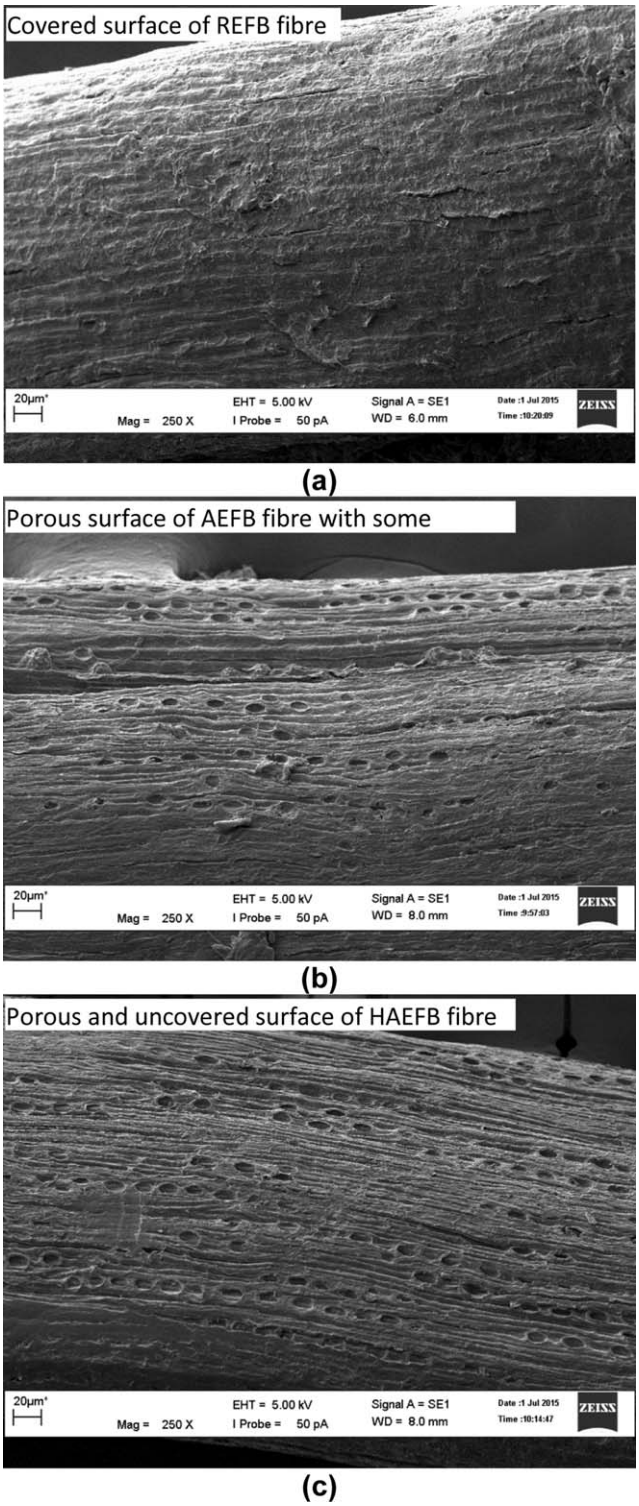


**Figure 5.** Scanning electron microscopy micrographs of the fibers: (a) REFB, (b) AEFB, and (c) HAEFB.

### Izod Impact Properties

The values of the impact strength (IS) of the composites are presented in Table II. The IS of RPP was found to be the maximum, whereas NFC showed the minimum. GF-based composite showed a comparatively higher value of 22.4 J/m$^2$. HC2 showed

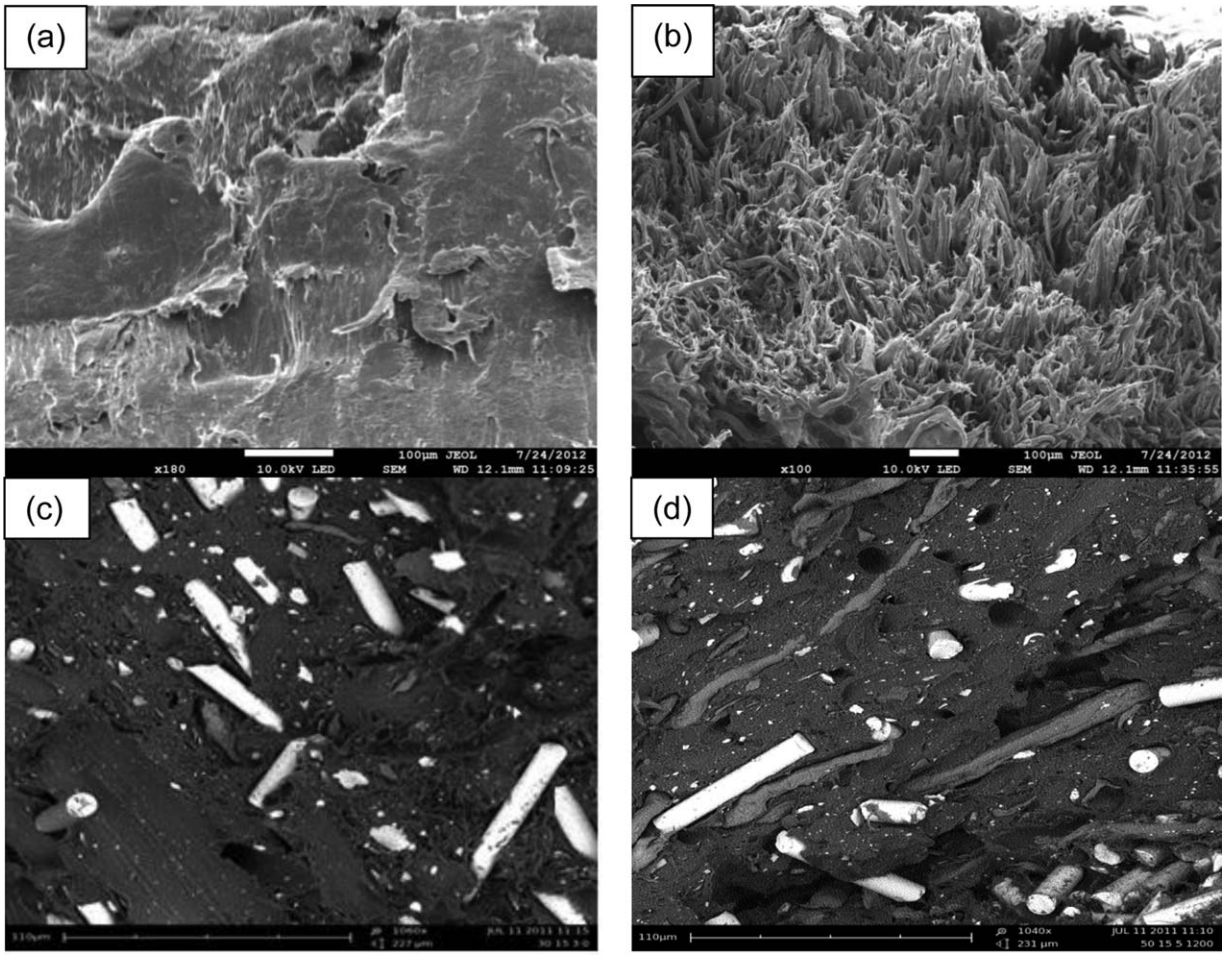


**Figure 6.** Field emission scanning electron microscopy micrographs of the fractured samples: (a) RPP, (b) NFC, (c) GFC, and (d) HC6.

the highest value of IS among the composites prepared with the alkali-treated EFB fibers (HC1 and HC3). On the other hand, the IS value was found to be increased with temperature during alkali treatment, and the maximum value was obtained for HC6. The increase in the IS value was probably due to the improved interfacial adhesion between the fiber and matrix. This adhesion was further improved because of the high-temperature treatment of the fibers in the alkaline solution. The trends of observed IS were consistent with the other mechanical properties. The improved properties of HCs were due to alkali and heated-alkali treatment, but an excess of alkali concentration caused the deterioration of the properties. Overall, IS was found to decrease after fiber loading as compared with that of RPP. This implied that the substitution of materials often involves the improvement of some properties with the simultaneous deterioration of others.

### Structural and Morphological Properties

The X-ray diffraction profiles of RPP and different composites are illustrated in Figure 4. The diffraction pattern of RPP revealed monoclinic α-phase crystals and showed peaks that were indexed as the (110), (040), (130), (041), and (060) planes.[21] Apart from these, the other sharp peaks in RPP profile probably arose from the unknown crystalline filler materials loaded previously in the recycled PP; we did not analyze them in this study because of their complexity. From the observed pattern, the crystal was apparently oriented along the *b* axis.[22] The profile of NFC contained wide peaks that came from previously indexed planes with a reduction in the peak intensity; this suggested that the untreated fibers inhibited crystal growth in RPP. Basically, natural fibers consist of amorphous parts because of the presence of lignin, pectin, wax, and hemicellulose, and their only crystalline part is cellulose, which usually shows peaks from the (110) and (002) planes.[6] From these two planes, diffused peaks were observed in the $2\theta$ regions from 15 to 18° and 21 to 23° due to the presence of amorphous components in the fibers. However, the treatment of fibers may have been able to remove these components and may have resulted in a higher crystalline cellulose content, which showed comparatively sharp peaks. As a result, in case of NFC, the peaks at $2\theta$ values of 14–22° were widened, whereas in case of GFC and HC, the peak intensity increased; this represented the fact that inclusion of GF improved the crystal growth. In case of HC2 and HC6, the intensity increased further. These results strongly indicate that the EFB fibers by treated alkali and heated-alkali solutions enhanced the crystal growth in RPP.

Careful observation of the increase in the intensity of the (110) plane of HC6, HC2, and HC from that of NFC and RPP convinced us to consider that the crystal growth of RPP by treated

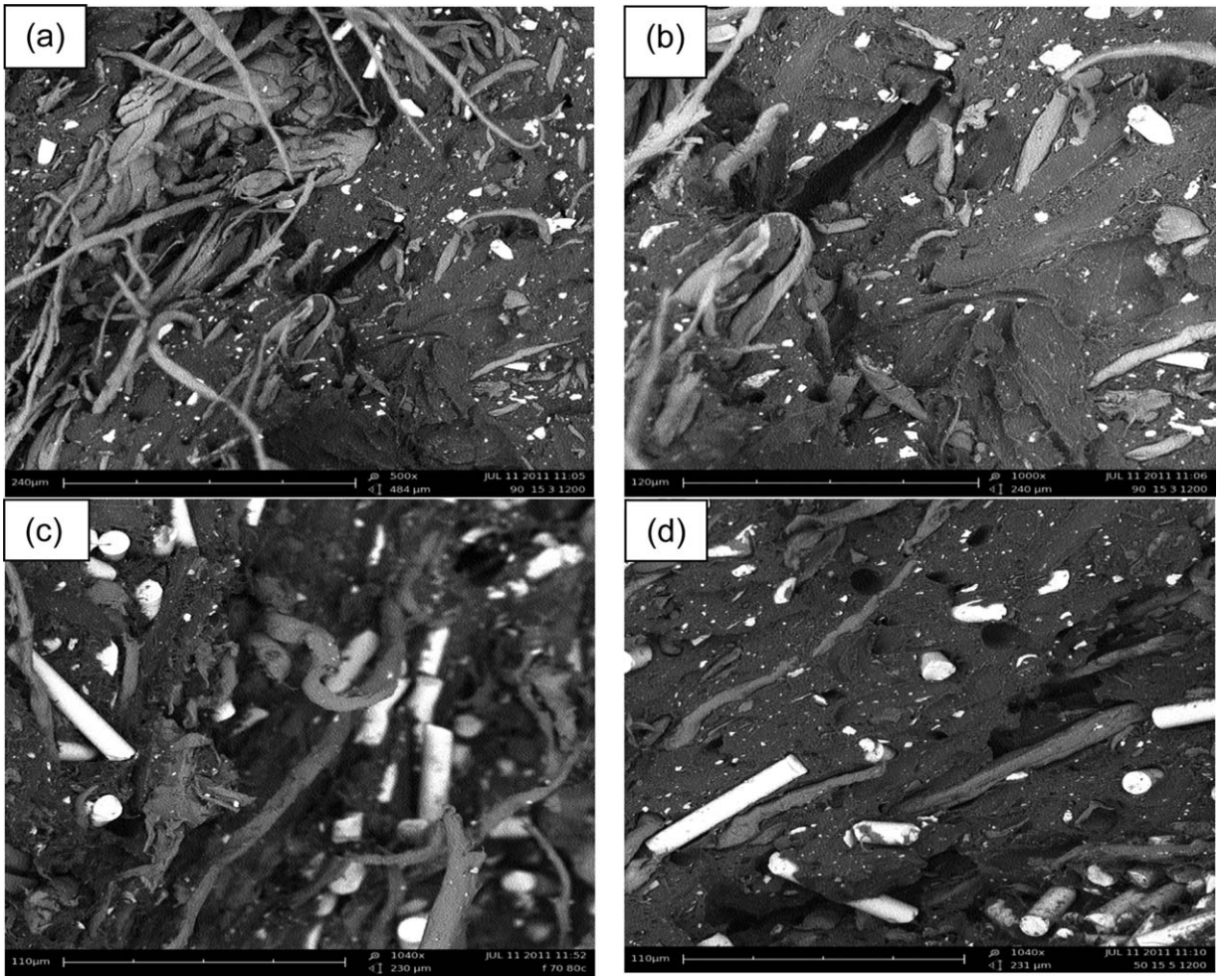


**Figure 7.** Field emission scanning electron microscopy micrographs of the fractured samples: (a) HC, (b) HC2, (c) HC5, and (d) HC6.

fibers not only occurred along the *b* axis but also along the *a* axis. Other important results from the X-ray diffraction profiles were that the peak width of the composites increased compared to that of RPP, and the peak position shifted slightly to lower angles. The increase in the peak width was assigned to the development of small crystallites. This was a reasonable result because of the presence of shredded fibers, which acted as many nucleating agents and may have interrupted the crystal growth and, thereby, resulted in small crystallites. The shift of the peak position to a lower angle was attributed to the increase in the lattice parameters; this may have arisen because of the distortion of crystal structures by the presence or intercalation of fiber components in the crystallites. Therefore, we suggest that the increase in the mechanical properties of the fiber-loaded composite was partially due to the increase in $\chi_{DSC}$ and the orientation of the crystals.

Figure 5 shows the scanning electron microscopy images of REFB [Figure 5(a)], AEFB [Figure 5(b)], and HAEFB [Figure 5(c)]. The surface of the raw fibers was covered by cementing materials, such as lignin, wax, and other surface impurities, which are clear in the image. On the other hand, alkali-treated fibers showed surfaces bearing some pores; this indicated the removal of those materials as the consequence of treatment. This surface was found to be more porous after it was treated with alkali and heat simultaneously, as shown in the image [Figure 5(c)]. The heat treatment of the fibers was enough to remove the noncellulosic materials. The exposure of the cellulose compound was favorable for good entanglement with the polymer matrix and may have improved the interfacial adhesion between the fibers and matrix in the presence of two types of coupling agents.

The surface micrographs of the fractured samples of the tensile specimen of RPP and various types of composites are displayed in Figures 6 and 7. Figure 6 shows the images of RPP, NFC, GFC, and HC6, whereas Figure 7 shows the surfaces of HC, HC2, HC5, and HC6. The surface of RPP was smooth, whereas the surfaces of NFC, GFC, and HC were relatively rough. The fiber pullout on the surfaces of these two samples was notable. In addition, voids were found on the surfaces of NFC, GFC, and HC. These were probably due to weak interfacial adhesion between the fiber and matrix. On the other hand, treated-fiber-based composites, such as HC2, HC5, and HC6, also showed fiber pullout, where the fibers were found to be broken down because of fracture and showed strong fiber–matrix interaction because of the alkali treatment of the fibers. To understand fiber

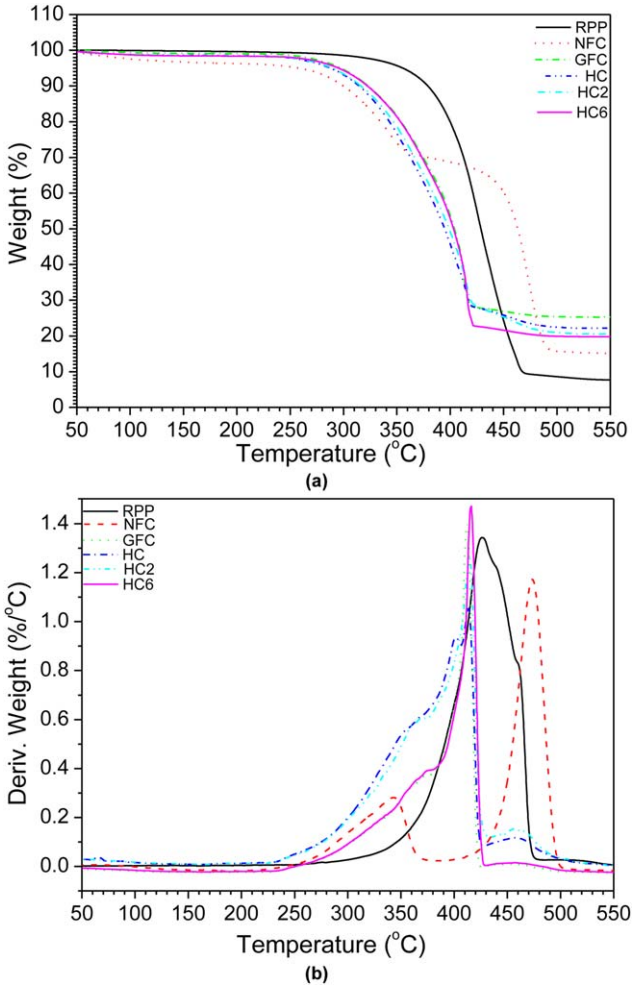


**Figure 8.** DSC thermograms of the various composites: (a) heating and (b) cooling cycles. [Color figure can be viewed in the online issue, which is available at wileyonlinelibrary.com.]

interaction, the amount of void formation in the original composites was calculated with the following equation[6]:

$$V_v = \left(\frac{d_{tc} - d_{ec}}{d_{tc}}\right) \quad (3)$$

where $V_v$ is the void fraction, $d_{tc}$ is the theoretical density, and $d_{ec}$ is the experimental density of the composites. The method of theoretical density calculation was explained in another article.[6] The numbers of voids for the EFB- and GF-based composites are included in Table II. We observed that the treated-fiber-based composites showed lower void contents than untreated ones. Fewer voids indicated strong interactions between the fiber and polymer. We expected that the removal of lignin and other surface impurities enhanced the adhesion between the fiber and matrix in the presence of two types of coupling agent.[6] Moreover, for all of the HCs, GFs were expectedly well dispersed throughout the composites; this resulted in low void contents between the fibers and polymers.

### Thermal Properties

The first heating and cooling cycles of the DSC thermograms of different samples are shown in Figure 8(a,b), respectively. We found that all of the samples exhibited two endothermic melting peaks around 125 and 160°C. The first melting peak ($T_{m1}$) and second melting peak ($T_{m2}$) were due to the PP copolymer and RPP, respectively.[6] $T_{m1}$ and $T_{m2}$ were very close to each other. Similarly, all of the samples exhibited two crystalline temperatures ($T_{c1}$ and $T_{c2}$) corresponding to the PP copolymer and RPP, respectively. The values of $T_{m1}$, $T_{m2}$, $T_{c1}$, and $T_{c2}$ are shown in Table III. The enhancements of $T_{m1}$ and $T_{m2}$ were found to be 1°C because of the incorporation of EFB fibers in both types of polymer. The values were found to be enhanced by 2°C because of the inclusion of treated fibers in all of the samples. Similarly, the enhancements of $T_{c1}$ and $T_{c2}$ with the incorporation of EFB fibers for both types of polymer were 1°C and that by treated was 4°C. We found that the crystallization started at a higher temperature in the composites comparted to that in RPP after they cooled from the melt state. In such cases, the order of $T_{c2}$ values could be arranged as follows HC6 > HC2 > HC > GFC > NFC > RPP. We expected that because of the presence of fibers, the RPP molecules had a low-energy configuration for the creation of nucleation sites and, thus, favored the RPP molecules to be oriented one by one to grow crystallites. The treated fibers had rougher surfaces that were more favorable for crystal growth. Hence, the RPP molecules started crystallization at higher temperatures. A similar explanation was applicable for $T_{c1}$.The heating enthalpies of the samples are presented in Table III. With these values and eq. (1), the $\chi_{DSC}$ values were calculated with a value of 209 J/g for 100% crystalline PP.[23] RPP showed a low $\chi_{DSC}$ value compared to the composites, which showed a gradual increase in $\chi_{DSC}$ because of fiber loading. The estimated maximum $\chi_{DSC}$ value from RPP and HC6 was 21%. Thus, natural fibers acted as good nucleating agents, and GFs acted as supplementary agents

**Table III.** Melting Points, Crystallization Temperatures, Enthalpies, and Crystallinities, Degradation Temperatures, and Residue Contents of the Samples

| Sample | $T_{m1}$ (°C) | $T_{m2}$ (°C) | $T_{c1}$ (°C) | $T_{c2}$ (°C) | Enthalpy (J/g) | $\chi_{DSC}$ (%) | $T_{max1}$ (°C) | $T_{max2}$ (°C) | Residue (wt %) |
|---|---|---|---|---|---|---|---|---|---|
| RPP | 125 | 161 | 118 | 127 | 46.58 | 22.3 | 426 | — | 7.5 |
| NFC | 126 | 162 | 119 | 128 | 28.44 | 22.6 | 344 | 473 | 15 |
| GFC | 127 | 162 | 119 | 128 | 28.42 | 22.2 | 369 | 408 | 25 |
| HC | 127 | 162 | 120 | 128 | 31.95 | 25.5 | 352 | 413 | 22 |
| HC2 | 127 | 163 | 121 | 130 | 33.12 | 26.4 | 366 | 413 | 21 |
| HC6 | 127 | 163 | 122 | 131 | 33.58 | 26.7 | 374 | 413 | 20 |

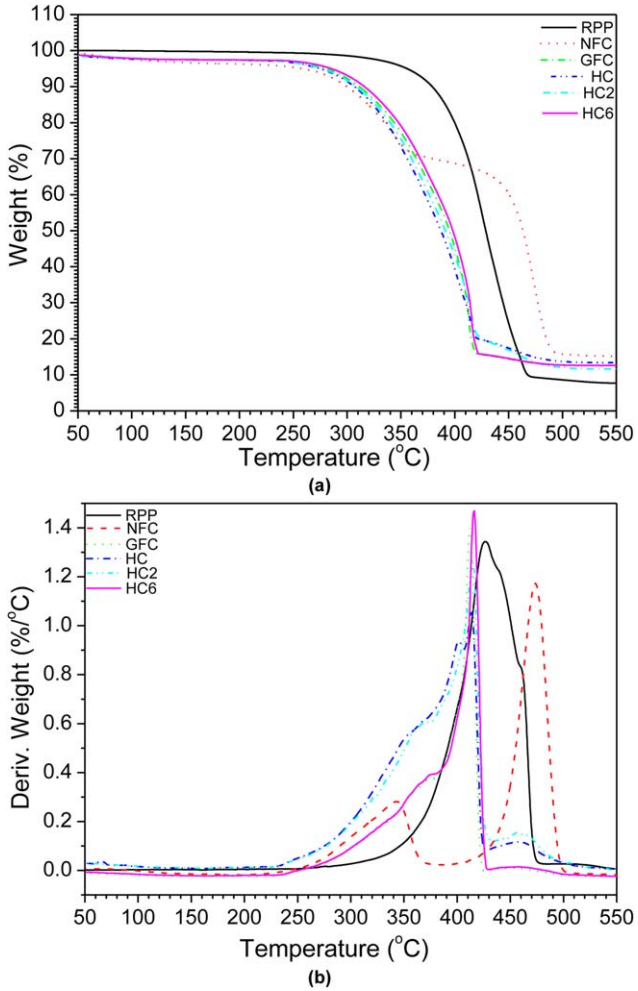


**Figure 9.** Thermograms of the different samples: (a) weight versus temperature and (b) derivative weight versus temperature. [Color figure can be viewed in the online issue, which is available at wileyonlinelibrary.com.]

for the crystallization in RPP. Such an increase in $\chi_{DSC}$ for fiber-based composites was reported elsewhere.[24]

The thermogravimetric analyses are illustrated in Figure 9, where weight versus temperature and derivative weight versus temperature are shown in Figure 9(a,b), respectively. We found that RPP degrades at one stage and its onset degradation temperature started around 426°C, whereas the composites degraded at two stage. The degradation temperatures from one stage ($T_{max1}$) and two stages ($T_{max2}$) were determined from Figure 6(b) and are presented in Table III. The $T_{max1}$ of NFC, HC, HC2 and HC6 was found to be increased gradually, whereas $T_{max2}$ for all these samples were almost same, except NFC and GFC. The increase in $T_{max1}$ is a thermal barrier effect of fibers whose presence delays RPP to be melted.[25] The high value of $T_{max1}$ for NFC suggests that it contains some components whose thermal barrier character is much higher than other components. Significant amount of residues were found to remain after completion of the degradation. Untreated EFB fiber based composite, NFC, showed residue of 15%, whereas GFC, HC, HC2 and HC6 HCs showed that in the range from 20 to 25%.

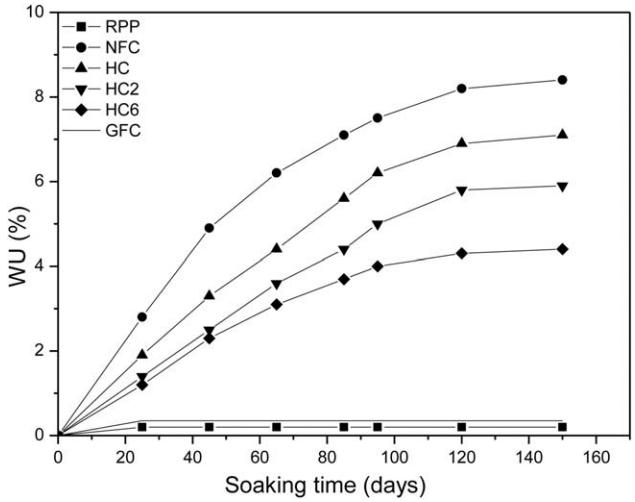


**Figure 10.** WU (%) by different composites.

### WU Properties

Figure 10 represents the WU trend of different composites at various soaking periods. WU depended on various parameters, including the type of fiber, its loading and orientation, area of the exposed surface, interfacial adhesion, voids, and surface protection.[26] We observed from the graph that the hydrophobic polymer matrix, RPP, absorbed a constant amount of water (0.2%) throughout the period of 150 days, whereas the EFB-fiber-based composite, NFC, absorbed the highest amount (8.4%) of water during the same period of immersion. The GF-based composite, GFC, showed a WU value of 0.35%. This was because of the completely hydrophobic nature of RPP and GF. On the other hand, HC absorbed 7.1% water during this period. However, the treatment of fibers reduced the water absorption of HC2 to a value of 5.9%, and temperature-aided alkali treatment (for the HC6) further reduced the value for HC6 to 4.4%. We found that all of the composites reached their saturation or equilibrium conditions after 150 days of soaking, and this indicated the Fickian model of diffusion.[27]

## CONCLUSIONS

HCs were prepared from RPP, GF, and EFB fibers in the presence of coupling agents (PB and FB). The effects of the alkali treatment and heat-aided alkali treatment of EFB fibers in terms of different mechanical, structural, thermal, and morphological properties of the composites were analyzed. The mechanical properties, including TS, TM, FS, and FM values, were found to increase considerably in the treated fibers when the heat-aided treatment fibers exhibited much improved properties. $\chi_{DSC}$ of RPP was found to increase more in the heat-aided alkali treated fibers than in the alkali-treated fibers. Both *a*- and *b*-axis-oriented $\alpha$ crystallites in RPP were formed by the treated fibers, whereas the virgin RPP and untreated EFB-reinforced HC showed only *b*-axis-oriented crystallites. The $\chi_{DSC}$ values of the treated-fiber-based composites increased, as calculated by the DSC enthalpies of the samples. We found that the double-axis-oriented RPP crystal in the composites showed enhanced mechanical and other performances. The heat-aided alkali-treated-fiber-loaded RPP composites showed more thermal stability than

the alkali-treated-fiber-based one. Additionally, the presence of coupling agents and GFs enhanced the properties of the HCs.

## REFERENCES


1. Dhakal, H. N.; Zhang, Z. Y.; Guthrie, R.; MacMullen, J.; Bennett, N. *Carbohydr. Polym.* **2013**, *96*, 1.
2. Ramesh, M.; Palanikumar, K.; Hemachandra, R. K. *Compos. B* **2013**, *48*, 1.
3. Islam, M. R.; Beg, M. D. H.; Gupta, A. *Bioresources* **2013**, *8*, 3753.
4. Alam, A. K. M. M.; Shubhra, Q. T. H.; Al-Imran, G.; Barai, S.; Islam, M. R.; Rahman, M. M. *J. Compos. Mater.* **2011**, *45*, 2301.
5. Islam, M. R.; Beg, M. D. H.; Gupta, A.; Mina, M. F. *J. Appl. Polym. Sci.* **2013**, *128*, 2847.
6. Islam, M. R.; Beg, M. D. H.; Mina, M. F. *J. Compos. Mater.* **2013**, *48*, 1887.
7. Islam, M. R.; Beg, M. D. H.; Gupta, A. *J. Thermoplast. Compos. Mater.* **2012**, *27*, 909.
8. Suhaimi, M. D. S. M.; Ismail, H. *Bioresources* **2014**, *9*, 7311.
9. van den Oever, M. J. A.; Snijder, M. H. B. *J. Appl. Polym. Sci.* **2008**, *110*, 1009.
10. Ramli, R.; Yunus, R. M.; Beg, M. D. H.; Islam, M. R. *J. Reinf. Plast. Compos.* **2011**, *30*, 5431.
11. Borysiak, S. *Polym. Bull.* **2010**, *64*, 275.
12. Sorrentino, L.; Simeoli, G.; Iannace, S.; Russo, P. *Compos. B* **2015**, *76*, 201.
13. Song, J. H. *Compos. B* **2015**, *79*, 61.
14. Yahaya, R.; Sapuan, S. M.; Jawaid, M.; Leman, Z.; Zainudin, E. S. *Mater. Des.* **2015**, *67*, 173.
15. Rivai, M.; Gupta, A.; Islam, M. R.; Beg, M. D. H. *Fiber Polym.* **2014**, *15*, 1523.
16. Adhikary, K. B.; Shusheng, P.; Staiger, M. P. *Chem. Eng. J.* **2008**, *142*, 190.
17. Alireza, A.; Nourbakhsh, A. *Waste Manage.* **2009**, *29*, 1291.
18. Lee, C. K.; Cho, M. S.; Kim, I. H.; Lee, Y.; Nam, J. D. *Macromol. Res.* **2010**, *18*, 566.
19. Chowdhury, M. N. K.; Beg, M. D. H.; Khan, M. R.; Mina, M. F. *Cellulose* **2013**, *20*, 1477.
20. Panthapulakkal, S.; Sain, M. *J. Appl. Polym. Sci.* **2007**, *103*, 2432.
21. Li, Y.; Pickering, K. L. *Compos. Sci. Technol.* **2008**, *68*, 3293.
22. Bhuiyan, M. K. H.; Rahman, M. M.; Mina, M. F.; Islam, M. R.; Gafur, M. A.; Begum, A. *J. Compos. A* **2013**, *52*, 70.
23. Garcia, M.; van Vliet, G.; Jain, S. *Adv. Mater. Sci.* **2004**, *6*, 169.
24. Jiang, Q.; Jia, H.; Wang, J.; Fang, E.; Jiang, J. *Iran. Polym. J.* **2012**, *21*, 201.
25. Liu, L.; Huang, Y. D.; Zhang, Z. Q.; Jiang, Z. X.; Wu, L. N. *Appl. Surf. Sci.* **2008**, 254, 2594.
26. Ellyin, F.; Maser, R. *Compos. Sci. Technol.* **2004**, *64*, 1863.
27. Rajkumar, G.; Srinivasan, J.; Suvitha, L. *Iran. Polym. J.* **2013**, *22*, 277.